Fracking

Naddia D. Arenas Zapata [a,b] Gabriela B. Savioli [a,*]
Patricia M. Gauzellino [b] Juan E. Santos [d,a,c]

[a] *Departamento de Energía, Instituto del Gas y del Petróleo , Universidad de Buenos Aires, Av. Las Heras 2214 Piso 3 C1127AAR Buenos Aires, Argentina.*

[b] *Facultad de Ciencias Astronómicas y Geofísicas, Universidad Nacional de La Plata, Paseo del Bosque s/n, B1900FWA, La Plata, Argentina.*

[c] *Department of Mathematics, Purdue University, 150 N. University Street, West Lafayette, Indiana, 47907-2067, USA.*

[d] *School of Earth Sciences and Engineering, Hohai University, Nanjing 211100, China.*

---

* Corresponding author.
E-mail address: gsavioli@fi.uba.ar (G. B. Savioli).

Abstract

The numerical fracking modeling combines a multiphase flow simulator for fluid injection with a fracking generation criteria. The procedure consists of injecting water into a gas shale reservoir to increase pore preasure until reaching a threshold defined in terms of a spatial distribution of weakness zones. A given computational cell is fractured by changing its porosity and permeability when the the threshold is attained.

The multiphase flow simulator uses the Black Oil formulation for two-phase fluid flow, which equations are solved using the IMPES algorithm. The weakness zones are defined in terms of the local vertical, horizontal and tectonic stresses.

Once a given stage of the fracking procedure is completed, the well is opened to flow to start production, taking into account the initial water backflow. The numerical examples illustrate both the fracking and production stages of the modeling procedure.

Keywords: Hydraulic fracturing, multiphase flow, numerical modeling, hydrocarbon production.

1 Introduction

Hydraulic fracturing is a standard procedure used to allow hydrocarbon production in tight gas and shale oil and gas reservoirs. It consist on injecting water mixed with sand or ceramic materia in the formation at high pressures in order to generate paths where hydrocarbons can flow to production wells. In this fashion new fractures are added to pre-existing natural ones enhancing the absolute permeability of the reservoir. Generally, this procedure generates bi-wing and planar fractures, normal to the minimum principal stresses.

To simulate one stage of the fracking procedure, the numerical model combines a two-phase flow simulator, based in the Black-Oil formulation [**?**,**?**], to represent fluid injection with a breakdown criterion that follows the formation weakness zones. The flow simulator is run until the pressure reaches a threshold breakdown value at a given computational cell. Then such cell and its neighbours are fractured, i. e. their permeability and porosity are increased with prescribed values. This, in turn, induces an inmediate pressure decay in the formation.

Once the planar fracture is completed, the two-phase simulator is applied to predict hydrocarbon production. At early times part of the injected water flows back before the hydrocarbon starts to be produced.

Among other approaches to numerical simulate hydraulic fracturing we mention [**?**], presenting a fully coupled thermal hydro-mechanical model and [**?**] analyzing a shale gas reservoir with large amounts of natural fractures. Furthermore, Lee et al [**?**] present a genetic algorithm to optimize the design of hydraulic fracturing scenarios.

2 The numerical hydraulic fracture procedure

The injection and production flow numerical model uses the Black-Oil formulation to two-phase, two component fluid flow allows the gas component to dissolve in the water phase. These equations are obtained by combining the mass conservation equation for each component with the two-phase Darcy's law [**?**]. To discretize the Black-Oil equations we use the public domain BOAST simulator (Fanchi, 1997), that solves the system using IMPES finite difference technique. Thus, a CFL time step needs to be imposed [**?**].

The fracture criterium to increase porosity and permeability at a given computational cell is defined in terms of a threshold pressure value P_{bd} defined as [**?**].

$$P_{bd} = 3\sigma_{Hmin} - \sigma_{Hmax} + T_0 - p_H, \tag{1}$$

where T_0 is the tensile stress of the rock, p_H the hydrostatic pressure and

$$\sigma_{Hmax} = \sigma_{Hmin} + \sigma_{Tect}, \tag{2}$$

with σ_{Tect} being the tectonic stress contribution, σ_{Hmax} and σ_{Hmax} the maximum and minimum horizontal stresses, respectively, obtained as

$$\sigma_{Hmin} = \frac{\nu}{1-\nu}\sigma_V, \quad \sigma_V = g\int_0^H \rho_f \, dH, \tag{3}$$

where H is the formation depth, ν the Poisson ratio, ρ_f the formation density and g the gravity constant.

3 Numerical Results

<< Figure 1 >>

<< Figure 2 >>

<< Figure 3 >>

<< Figure 4 >>

4 Conclusions

5 Aknowledgements

The work of J. E. Santos was partially funded by the GRANT PIP 112-20080100952 from CONICET, Argentina.

References

[1] Schoenberg, M., and Douma, J., Elastic wave propagation in media with parallel fractures and aligned cracks, Geophys. Prosp., 36, 571-590, 1988.

[2] Gurevich, B., Elastic properties of saturated porous rocks with aligned fractures, J. Appl. Geophys., 54, 203-218, 2003

[3] Grechka, V., Comparison of the non-interaction and differential schemes in predicting the effective elastic properties of fractured media: International J. of Fracture, 144, 181-188, 2007.

[4] Picotti, S., Carcione, J. M., Gei, D., Rossi, G., and Santos, J. E., Seismic modeling to monitoring CO_2 geological storage. The Atzbach-Schwanenstadt gas field, J. Geophys. Res., 117, B06103, 2012.

[5] Grechka, V., and Kachanov, M., Effective elasticity of rocks with closely spaced and intersecting cracks: Geophysics, 71, D85-D91, 2006.

[6] Grechka, V., and Kachanov, M., 2006, Effective elasticity of fractured rocks: A snapshot of the work in progress: Geophysics, 71, W45-W58, 2006.

[7] Saenger E. H., Ciz, R., O. S. Krüger, O. S., Schmalholz, S. M., Gurevich, B., and Shapiro, S. A., Finite-difference modeling of wave propagation on microscale: A snapshot of the work in progress, Geophysics, 72, SM293-SM300, 2007.

[8] Wenzlau, F., Altmann, J. B., and Müller, T. M., Anisotropic dispersion and attenuation due to wave-induced flow: quasi-static finite element modeling in poroelastic solids, J. Geophys. Res., 115, B07204, doi:10.1029/2009JB006644, 2010.

[9] Carcione, J. M., Gurevich, B., and Santos, J. E., and Picotti, S., Angular and frequency dependent wave velocity and attenuation in fractured porous media, Pure Appl. Geophys., DOI 10.1007/s00024-012-0636-8, 2013.

[10] White, J. E., Mikhaylova, N. G., and Lyakhovitskiy, F. M., Low-frequency seismic waves in fluid saturated layered rocks, Physics of the Solid Earth, 11, 654-659, 1975.

[11] Gelinsky, S., and Shapiro, S. A., Poroelastic Backus-averaging for anisotropic, layered fluid and gas saturated sediments, Geophysics, 62, 1867-1878, 1997.

[12] Krzikalla, F. and Müller, T., Anisotropic P-SV-wave dispersion and attenuation due to interlayer flow in thinly layered porous rocks, Geophysics, 76, W 135; doi:10.1190/1.3555077, 2011.

[13] Carcione, J. M., Santos, J. E. and Picotti, S., Anisotropic poroelasticity and wave-induced fluid flow. Harmonic finite-element simulation, Geophys. J. Internat., 186, 1245-1254, 2011.

[14] Picotti, S., and Carcione, J. M., Santos, J. E., and Gei, D., Q-anisotropy in finely-layered media, Geophys. Res. Lett., 37, L06302, 2010.

[15] Santos, J. E., Rubino, J. G., and Ravazzoli, C. L., A numerical upscaling procedure to estimate effective bulk and shear moduli in heterogeneous fluid-saturated porous media, Comput. Methods Appl. Mech. Engrg., 198, 2067-2077, 2009.

[16] Santos, J. E., Carcione, J. M., and Picotti, S., Viscoelastic-stiffness tensor of anisotropic media from oscillatory numerical experiments, Comput. Methods Appl. Mech. Engrg., 200, 896-904, 2011.

[17] Carcione, J.M., 2007. Wave fields in real media: wave propagation in anisotropic, anelastic, porous and electromagnetic media, in Handbook of Geophysical Exploration, 2nd edn, Vol. 38, 515pp., eds Helbig, K. & Treitel, S., Elsevier, Oxford.

[18] Carcione, J. M., Anisotropic Q and velocity dispersion of finely layered media. Geophys. Prosp., 40, 761-783, 1992.

[19] Raviart, P. A., and Thomas, J. M., Mixed finite element method for 2nd order elliptic problems, Mathematical Aspects of the Finite Element Methods, Lecture Notes of Mathematics, vol. 606, Springer, 1975.

[20] Krief, M., Garat, J. Stellingwerff, J. and Ventre, J., A petrophysical interpretation using the velocities of P and S waves (full waveform sonic), The Log Analyst, 31, 355-369, 1990.

[21] Carcione, J. M., Gurevich, B., and Cavallini, F., A generalized Biot-Gassmann model for the acoustic properties of shaley sandstones, Geophys. Prosp., 48, 539-557, 2000.

[22] Gurevich, B., Zyrianov, V. B, and Lopatnikov, S. L., Seismic attenuation in finely layered porous rocks: Effects of fluid flow and scattering, Geophysics, 62, 319-324, 1997.

[23] Carcione, J. M., Santos, J. E., and Picotti, S., Fracture induced anisotropic attenuation, Rock Mech. Rock Engrg., 45, 929-942, 2012.

[24] Russo, D., and Bouton, M., Statistical analysis of spatial variability in unsaturated flow parameters, Water Res. Res., 28, 1911-1925, 1992.

[25] Russo, D., Russo, I., and Laufer, A., On the spatial variability of parameters of the unsaturated hydraulic conductivity, Water Res. Res., 33, 945-956, 1997.

List of Figures

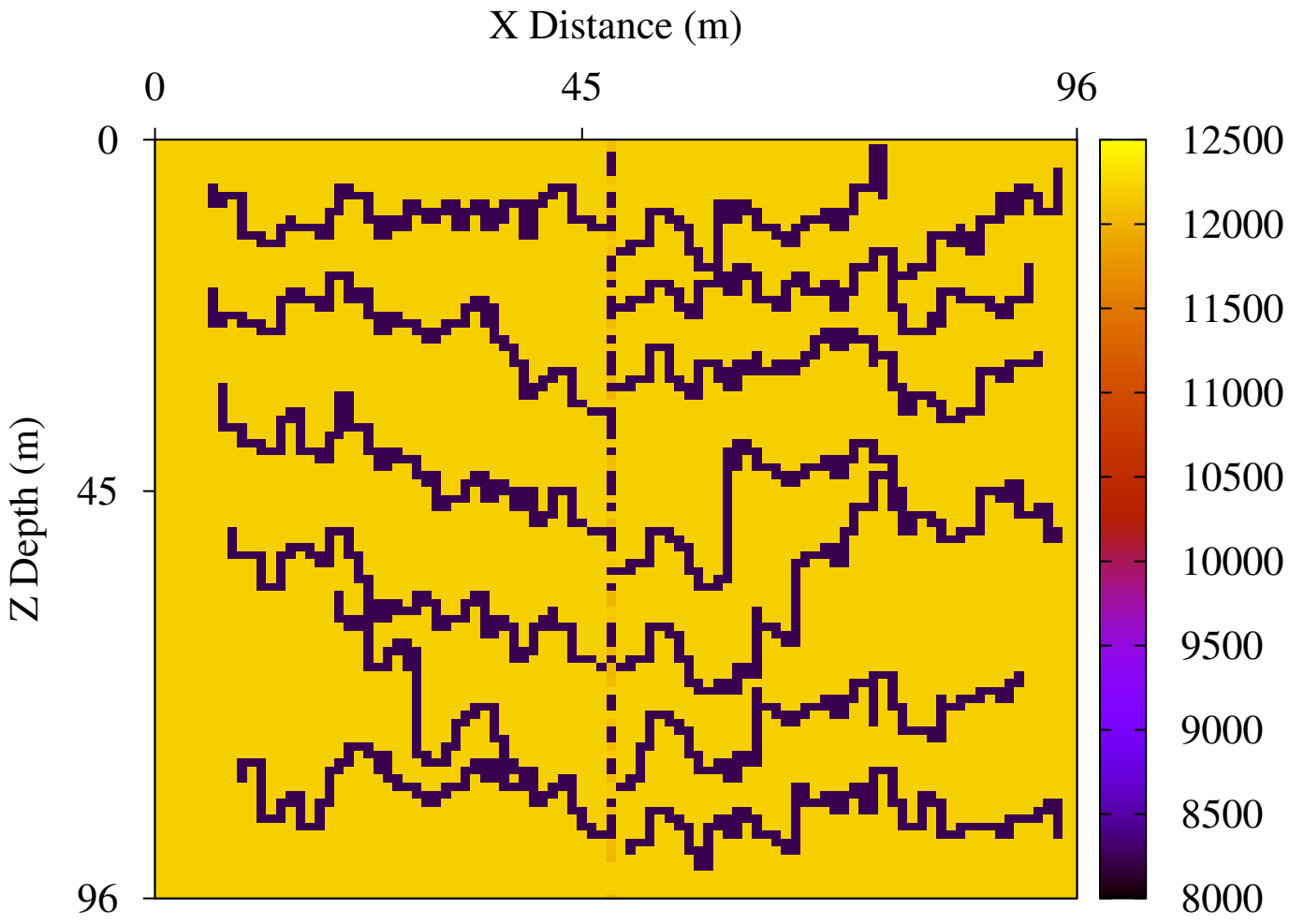

Fig. 1. Threshold pressure map (MPa)-PASAR A MPA!!!

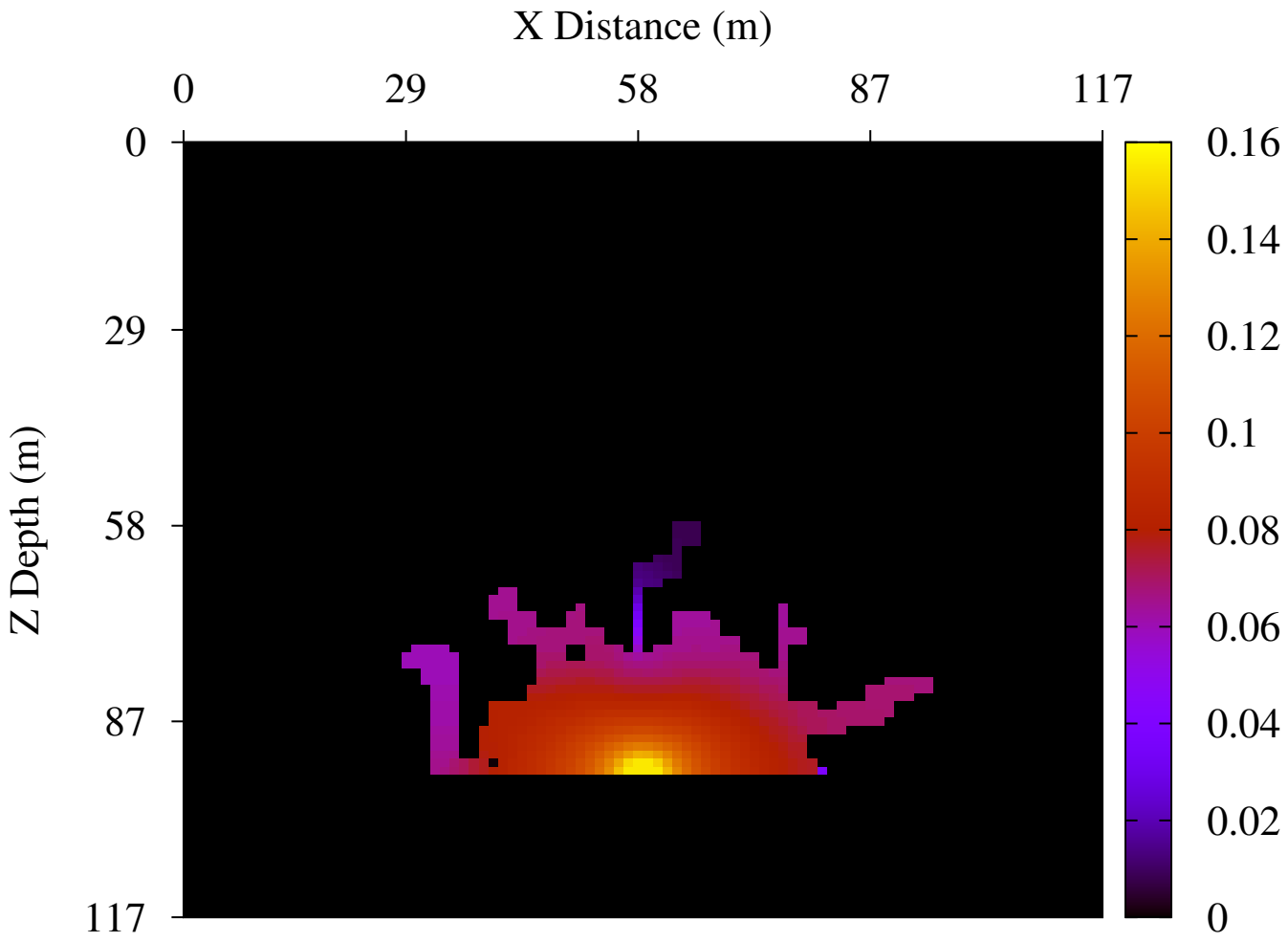

Fig. 2. Normalized injected fluid pressure after after 40 minutes of injection- CHEQUEAR TIEMPO!!

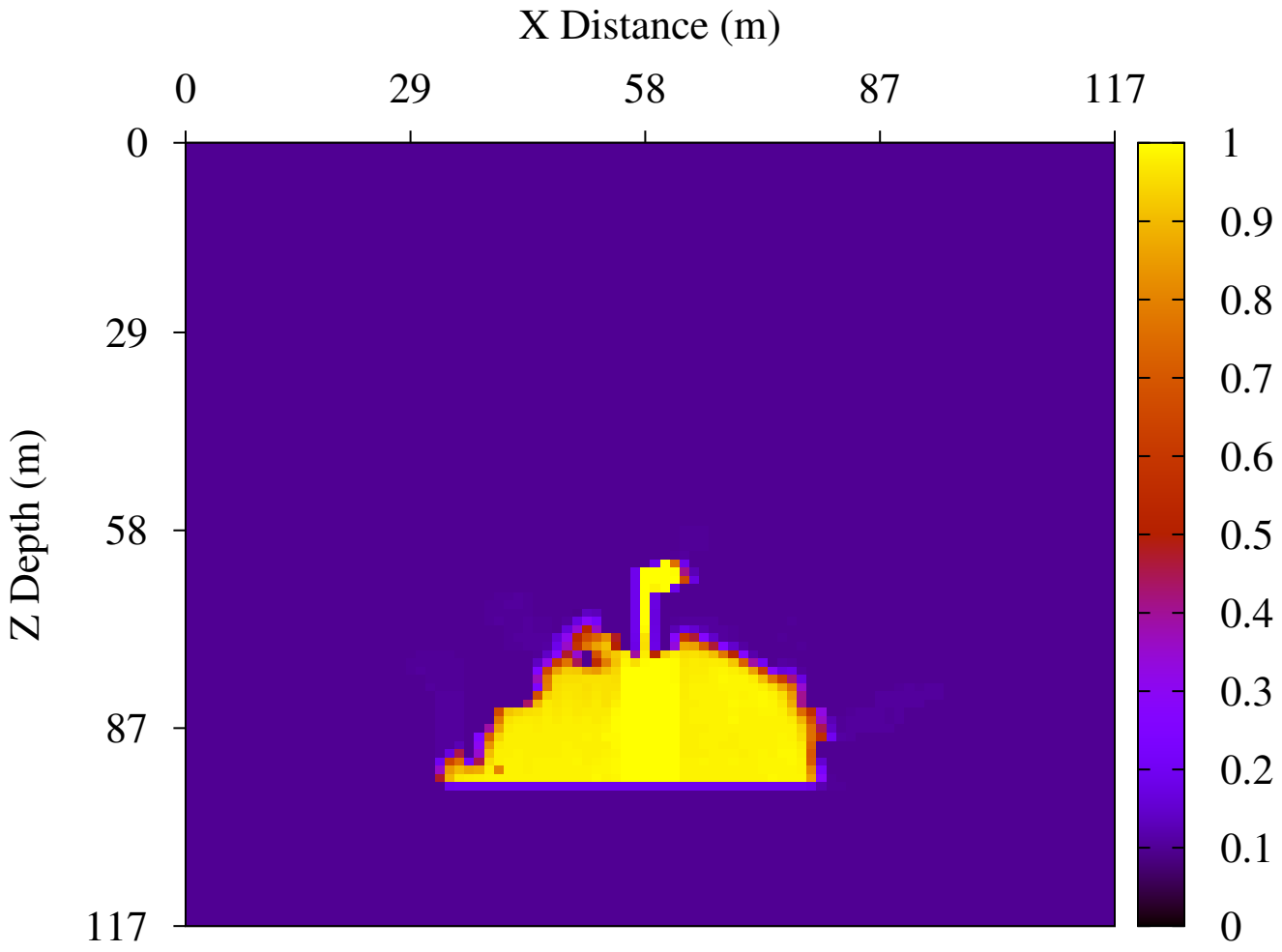

Fig. 3. Injected fluid saturation after 40 minutes of injection- CHEQUEAR TIEMPO!!

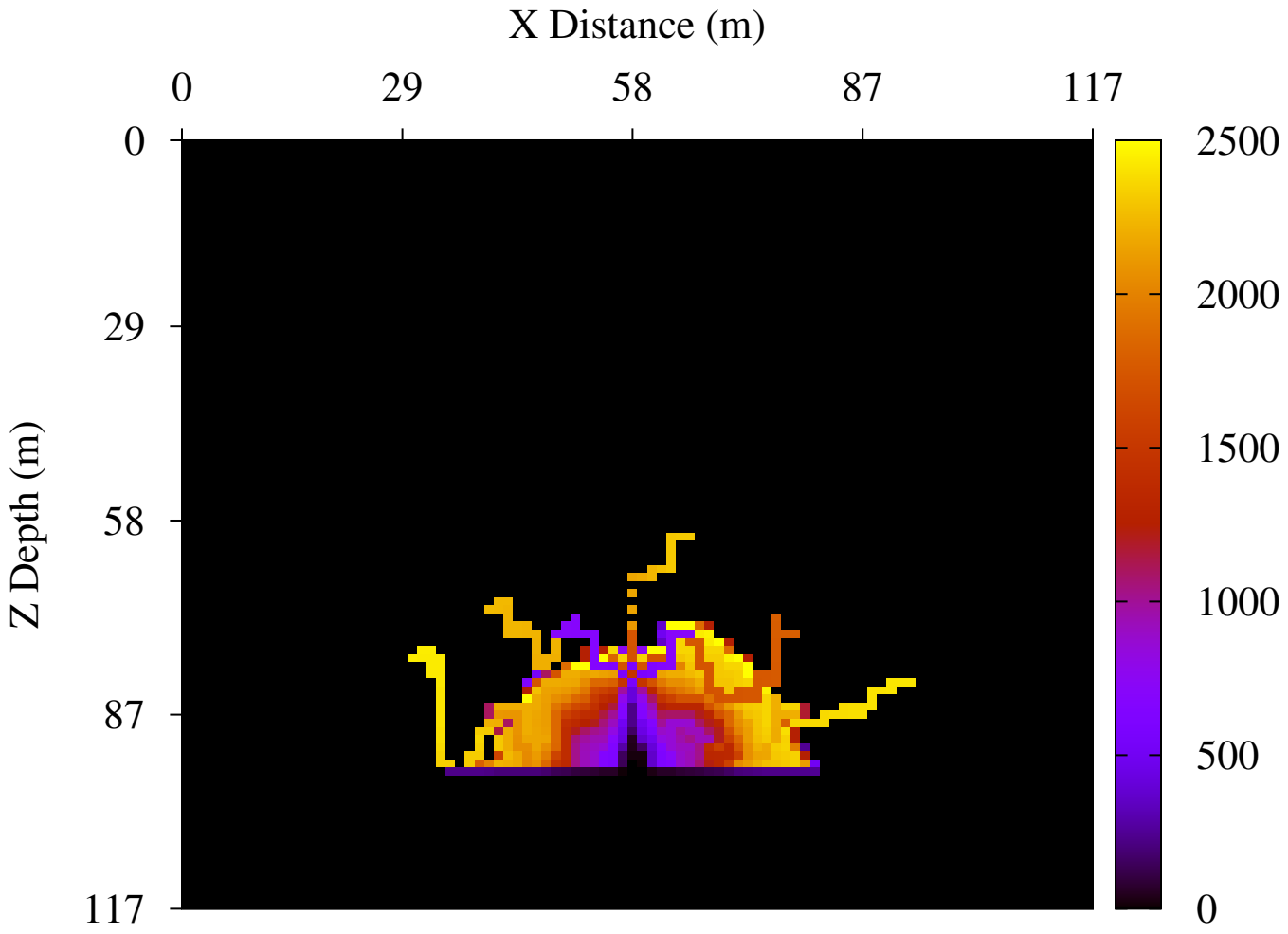

Fig. 4. Breakdown times map after 40 minutes of injection- CHEQUEAR TIEMPO!!

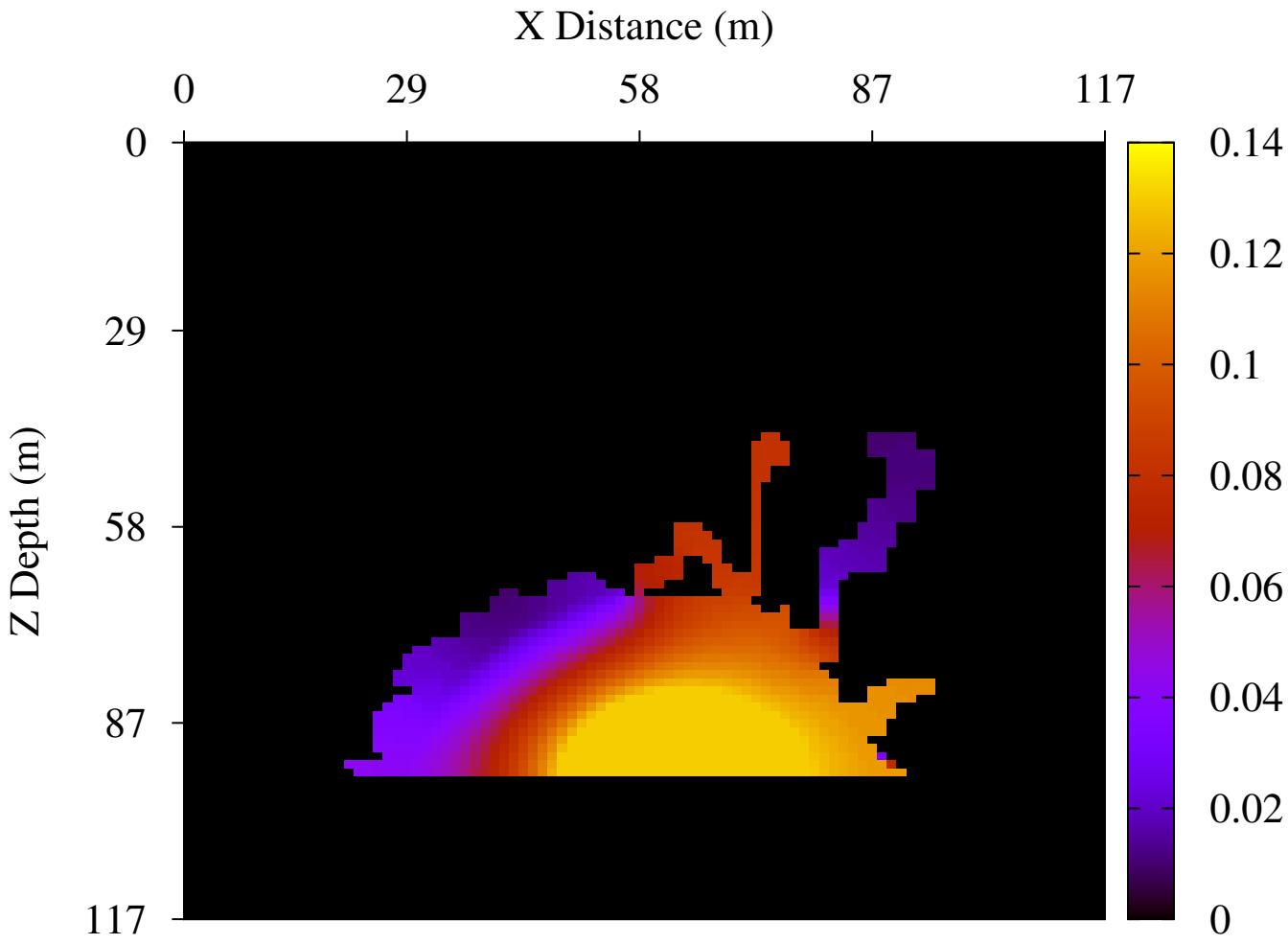

Fig. 5. Normalized injected fluid pressure after after 60 minutes of injection-CHEQUEAR TIEMPO!!

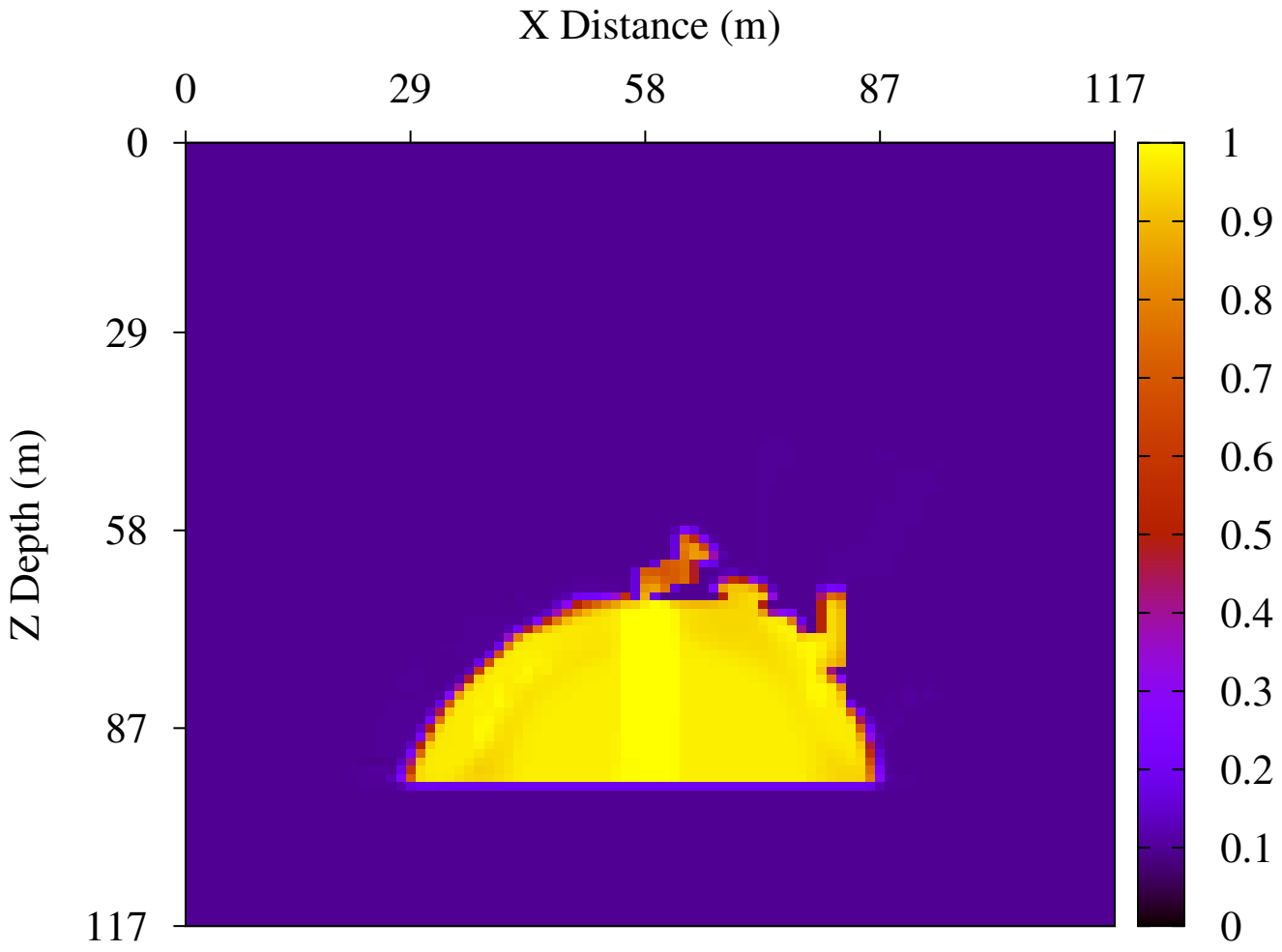

Fig. 6. Injected fluid saturation after 60 minutes of injection- CHEQUEAR TIEMPO!!

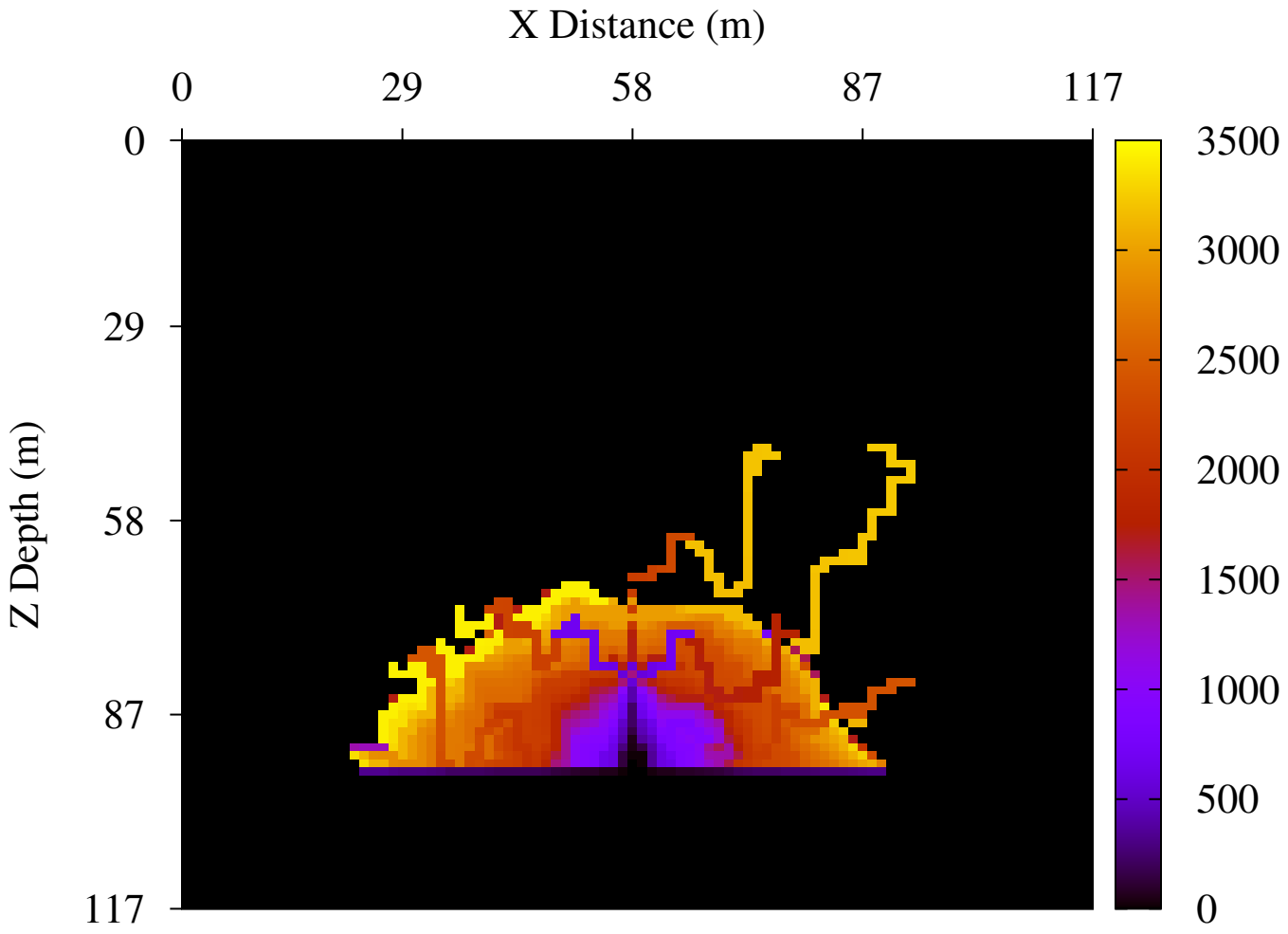

Fig. 7. Breakdown times map after 60 minutes of injection- CHEQUEAR TIEMPO!!

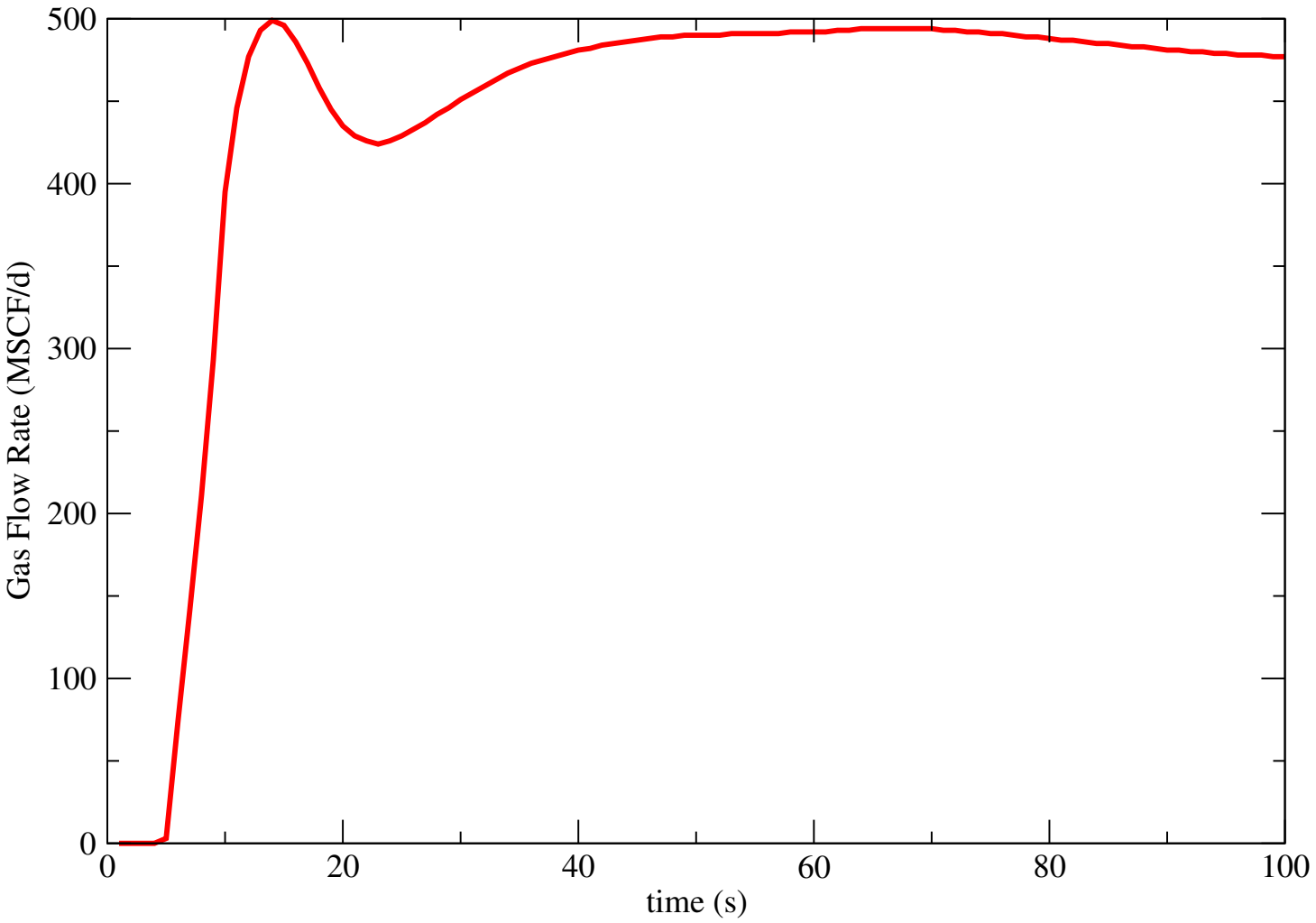

Fig. 8. Gas production rate MSCF/d- CHEQUEAR TIEMPO y ELEGIR UNIDADES!!

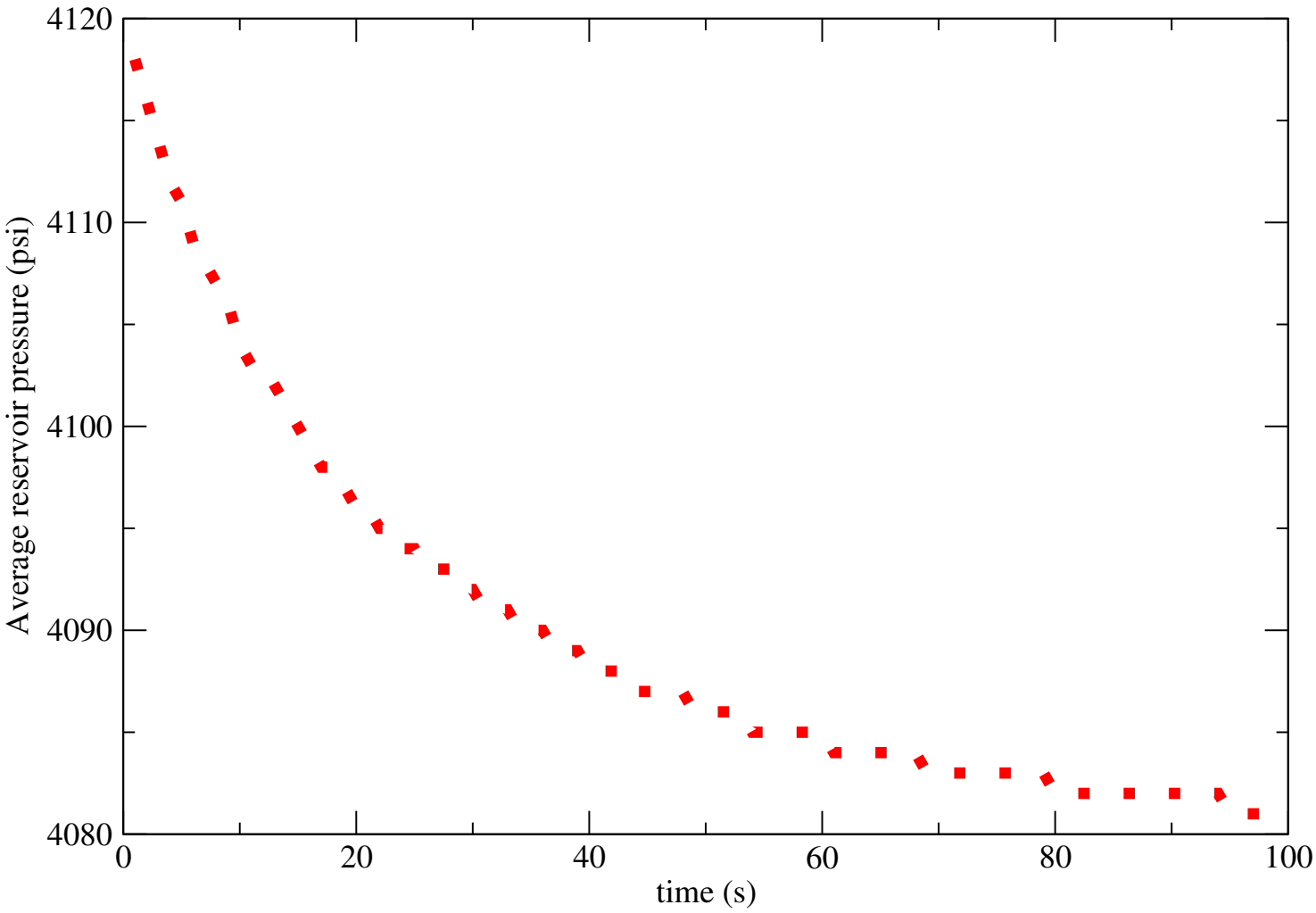

Fig. 9. Average produced fluids pressure, psi- CHEQUEAR TIEMPO y ELEGIR UNIDADES!!